IEEE Journal of Microwaves

Received 5 May 2023; revised 11 August 2023; accepted 4 September 2023. Date of publication 22 September 2023; date of current version 9 October 2023.

Digital Object Identifier 10.1109/JMW.2023.3313111

A Survey of GaN HEMT Technologies for Millimeter-Wave Low Noise Applications

NICHOLAS C. MILLER [1] (Senior Member, IEEE), ANDREA ARIAS-PURDUE [2] (Member, IEEE), ERDEM ARKUN [3] (Member, IEEE), DAVID BROWN [4] (Member, IEEE), JAMES F. BUCKWALTER [5] (Fellow, IEEE), ROBERT L. COFFIE [6] (Senior Member, IEEE), ANDREA CORRION [3] (Member, IEEE), DANIEL J. DENNINGHOFF [3] (Member, IEEE), MICHAEL ELLIOTT [7], DAVE FANNING [3] (Senior Member, IEEE), RYAN GILBERT [7], DANIEL S. GREEN [5] (Member, IEEE), FLORIAN HERRAULT [5] (Senior Member, IEEE), BEN HEYING [6], CASEY M. KING [2] (Member, IEEE), EYTHAN LAM [8] (Member, IEEE), JEONG-SUN MOON [3] (Fellow, IEEE), PETRA V. ROWELL [2] (Member, IEEE), GEORGES SIDDIQI [3] (Member, IEEE), IOULIA SMORCHKOVA [6], JOE TAI [3], JANSEN UYEDA [6], AND MIKE WOJTOWICZ [6]

(Regular Paper)

[1]Air Force Research Laboratory Sensors Directorate, Wright-Patterson AFB, OH 45433-7131 USA
[2]Teledyne Scientific, Thousand Oaks, CA 91360-2362 USA
[3]HRL Laboratories, Malibu, CA 90265-4797 USA
[4]BAE Systems, Nashua, NH 03060-6909 USA
[5]Pseudolithic, Santa Barbara, CA 93105-1914 USA
[6]Northrop Grumman Corporation, Redonda Beach, CA 90278-1001 USA
[7]KBR, Wright-Patterson AFB, OH 45433-7131 USA
[8]University of California, Santa Barbara, Santa Barbara, CA 93106-9010 USA

CORRESPONDING AUTHOR: Nicholas C. Miller (e-mail: nicholas.miller.58@us.af.mil).

This work was supported by the Air Force Research Laboratory under Award FA807518D0015.

ABSTRACT This article presents a set of measured benchmarks for the noise and gain performance of six different millimeter-wave (mm-wave) gallium nitride (GaN) high electron mobility transistor (HEMT) technologies fabricated at four different foundries in the United States. Measurements of the GaN transistors were collected on two independent noise parameter (NP) systems from 8–50 GHz and 75–110 GHz. The resulting raw NPs were stitched together to yield ultra broadband 8–110 GHz smoothed NPs. Several comparisons and summaries of the minimum noise figure and associated gain are reported for the six different GaN technologies. This work seeks to provide an initial database for noise and gain of GaN HEMTs at mm-wave frequencies to quantify progress on technology in the future.

INDEX TERMS Gallium nitride (GaN), high electron mobility transistor (HEMT), noise parameters, low noise amplifier.

I. INTRODUCTION

Gallium nitride (GaN) high electron mobility transistors (HEMTs) offer superior performance for radio frequency (RF) power amplifier (PA) applications due to their high voltage and current capabilities at higher frequencies [1]. Recently, GaN HEMTs have become attractive for low noise amplifier (LNA) applications. Compared to high-performing low-noise technologies including gallium arsenide and indium phosphide, GaN HEMTs offer considerably higher breakdown voltages while maintaining good noise figure (NF) and gain [2]. The high breakdown voltage is particularly important for transceivers as GaN-based LNAs can withstand higher input power levels. This eliminates the need for RF input limiters which increases the receiver's overall NF and size and complexity of the chips [2], [3], [4].

Several high linearity Ka-band GaN LNAs for 5 G applications have been shown in literature. In [5], a 100 nm GaN on Si LNA demonstrated a gain of 19.5–22.5 dB from 23–30 GHz

with a 0.4–1.1 dB NF and OP1dB of about 20.8 dBm. Another work in the same technology has shown a gain of 26 dB from 33–38 GHz with a 2 dB NF and OP1dB of 20 dBm [6]. A 90 nm GaN LNA demonstrated a gain of 14.3–24.4 dB from 18–44 GHz with a 1.5–2.5 dB NF [7]. A 150 nm GaN on SiC LNA measured a gain of 15–17 dB from 25–31 GHz with a 2.2 dB NF and OP1dB of 17.4 dBm [8]. A previously reported LNA in 40 nm GaN had also shown 1–1.6 dB NF at 30–39.3 GHz with OP1dB of 11 dBm [9].

GaN-based LNA demonstrations operating at millimeter-wave (mm-wave) frequencies have also recently gained considerable attention as scaled-gate GaN HEMT technologies continue to evolve and mature. A 100 nm GaN-on-SiC LNA obtained a 2.9–5 dB NF and >20 dB gain at 86–98 GHz [2]. In [3], a 90 nm GaN-on-SiC LNA achieved 3.5–4.2 dB NF and 15.5–16.1 dB gain from 75–83 GHz and 3.3–3.8 dB NF and 18–19.1 dB gain from 91–96 GHz. A 70 nm GaN-on-SiC LNA reported 2.8–3.3 dB NF and 21–24 dB gain across a broad 63–101 GHz frequency range [10]. A 60 nm GaN-on-Si LNA exhibited 4.4–5.5 dB NF from 90–95 GHz [4]. There exists several other mm-wave GaN-based LNA demonstrations in the literature including a 120 nm GaN-on-SiC LNA [11], a 100 nm GaN-on-Si LNA [12], and other 100 nm GaN-on-SiC LNAs [13], [14]. An excellent review of V- and W-band GaN LNAs is presented in [15].

A critical aspect of first-pass design success of mm-wave GaN-based LNAs is the accuracy of the noise models employed in the circuit simulators. Accurate models require precision measurements of the GaN HEMT technologies. However, as the frequency of interest increases into the mm-wave range, measurement systems which can collect noise data become rare. This becomes evident by investigating the measurement and modeling of the individual transistors used for GaN-based LNA designs in the literature. In [3], a 90 nm GaN HEMT was characterized and modeled across a lower 2–50 GHz frequency range and was used to project modeled performance and design the LNAs from 75–83 GHz and 91–95 GHz. The 63–101 GHz GaN-based LNA in [10] was designed using small-signal models extracted from S-Parameter measurements up to 225 GHz, but the noise models were extracted from on-wafer noise parameter (NP) measurements from 8–50 GHz. It is clear from these two examples that NP measurements collected on GaN HEMT technologies in the upper mm-wave frequency ranges are rare in the literature.

This article seeks to provide quantitative benchmarks for the noise and gain performances of mm-wave GaN HEMT technologies. Broadband NP measurements from 8–50 GHz and 75–110 GHz were collected on a total of six different mm-wave GaN HEMT technologies fabricated at four independent foundries in the United States. The raw NPs collected on the individual test benches were merged and processed together to yield ultra broadband 8–110 GHz smoothed NPs. The article is organized as follows. Section II briefly describes the NP systems at the Air Force Research Laboratory (AFRL) Sensors Directorate RF measurement laboratory. Descriptions of the six different mm-wave GaN HEMT technologies are provided in Section III. In Section IV, a thorough summary and comparison of the mm-wave GaN HEMT measured noise and gain performances is presented. Section V provides conclusions for this mm-wave GaN HEMT survey.

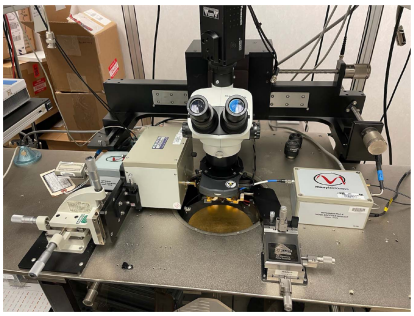

FIGURE 1. The 8–50 GHz NP system used to characterize the mm-wave GaN transistors. Photo by AFRL.

II. BROADBAND NOISE PARAMETER MEASUREMENTS

Critical transistor figures of merit for LNAs include NF and small-signal gain. In this survey, the NPs of mm-wave GaN transistors are analyzed to shed light on their potential performance in LNA applications. The standard representation of a transistor's noise factor is defined as

$$F = F_{\min} + \frac{4R_n}{Z_0}\frac{\left|\Gamma_S - \Gamma_{s,\text{opt}}\right|^2}{\left(1-|\Gamma_S|^2\right)\left|1+\Gamma_{s,\text{opt}}\right|^2}, \tag{1}$$

where $F_{\min}$ is the minimum noise factor, R_n is the equivalent noise resistance, and $\Gamma_{s,\text{opt}}$ is the optimum noise reflection coefficient [16]. In the remainder of this survey, the minimum NF, $\text{NF}_{\min} = 10\log_{10} F_{\min}$, of the mm-wave GaN transistors is analyzed. The associated gain is defined as the available gain evaluated at the optimum noise reflection coefficient [17]

$$G_{\text{assoc}} = \frac{|S_{21}|^2\left(1-\left|\Gamma_{s,\text{opt}}\right|^2\right)}{\left|1-S_{11}\Gamma_{s,\text{opt}}\right|^2\left(1-|\Gamma_{\text{out}}|^2\right)}, \tag{2}$$

where the output reflection coefficient is

$$\Gamma_{\text{out}} = S_{22} + \frac{S_{12}S_{21}\Gamma_{s,\text{opt}}}{1-S_{11}\Gamma_{s,\text{opt}}}. \tag{3}$$

NP measurements were collected for each mm-wave GaN HEMT technology at AFRL's RF measurement laboratory. The transistors were characterized on independent test benches which operate across broad 8–50 GHz and 75–105 GHz ranges. Both systems utilize the Maury Microwave "cold-only" NP measurement formulation [18] in the Automated Tuner System (ATS) Software. Fig. 1 illustrates the first test bench used to characterize the NPs across the 8–50 GHz frequency range. Components of this measurement system includes an Agilent 346 C Option:K01 1–50 GHz noise source, the Maury Microwave MT7553N50 noise switch module, a Maury MT984AU 8–50 GHz automated mechanical impedance tuner, a Maury MT7553B03 noise receiver module, an Agilent E5273 A source measure unit (SMU), and a Keysight N5273B PNA-X. The PNA-X

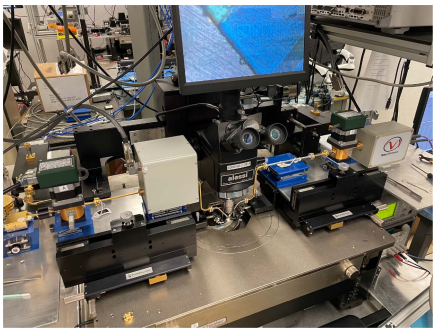

FIGURE 2. The W-band (75–110 GHz) NP system used to characterize the GaN transistors. Photo by AFRL.

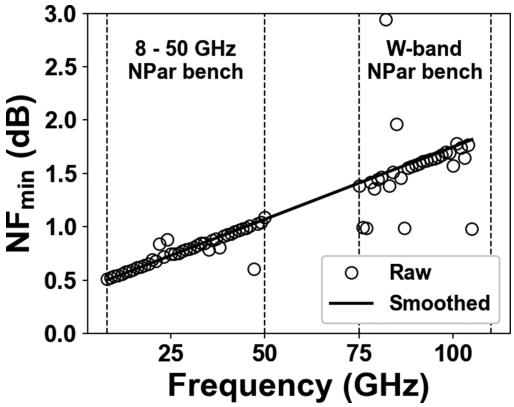

FIGURE 3. Raw NF_{min} (black circles) collected on the 8–50 GHz and 75–110 GHz NP measurements systems and the smoothed, continuous NF_{min} (solid line) processed from the raw NP sets. The frequency bands of the two independent NP measurement systems are indicated with the vertical dashed lines.

is used as both a vector network analyzer and a NF meter in this system. FormFactor 50 GHz ACP probes and GGB 50 GHz picoprobes were used for probing the transistors. The W-band (75–110 GHz) NP measurement system is displayed in Fig. 2. The components of this system include a QuinStar QNS-FB15LW W-band noise source, two Flann 27333-3E W-band switches, a Maury MT979AL 75–110 GHz automated mechanical impedance tuner, a Maury MT7553M10 noise receiver module comprised of a W-band LNA and a mixer down-converter, two Virginia Diodes, Inc. WR-10 VNA extension modules, an Agilent E5273 A SMU, and a Keysight N5273B PNA-X. Again, the VNA and NFM features of the PNA-X are used in this measurement system. GGB WR-10 picoprobes were used to probe the transistors on the W-band system.

The following method was employed to synthesize NPs across the ultra broadband 8–110 GHz frequency range. First, the raw NPs were measured on both independent test benches and the resulting ATS files were saved to disk. The raw NP data files were then merged and loaded into the Maury ATS software. Then, the complete data sets were processed using a standard ATS procedure to generate smoothed NPs across the 8–110 GHz frequency range. Figs. 3–6 present an example

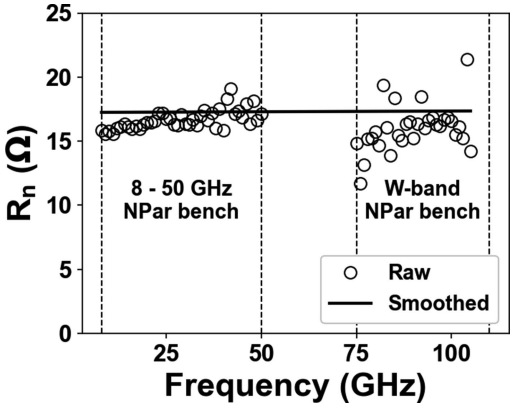

FIGURE 4. Raw R_n (black circles) collected on the 8–50 GHz and 75–110 GHz NP measurements systems and the smoothed, continuous R_n (solid line) processed from the raw NP sets. The frequency bands of the two independent NP measurement systems are indicated with the vertical dashed lines.

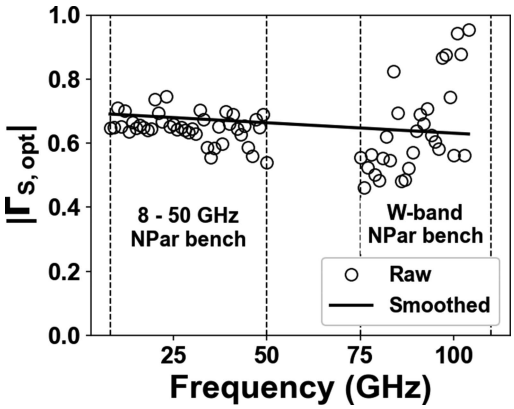

FIGURE 5. Raw $|\Gamma_{s,opt}|$ (black circles) collected on the 8–50 GHz and 75–110 GHz NP measurements systems and the smoothed, continuous $|\Gamma_{s,opt}|$ (solid line) processed from the raw NP sets. The frequency bands of the two independent NP measurement systems are indicated with the vertical dashed lines.

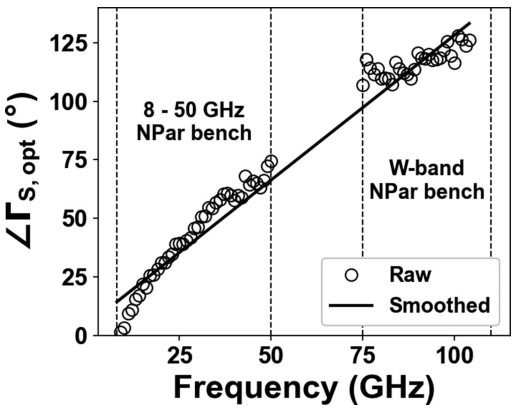

FIGURE 6. Raw $\angle\Gamma_{s,opt}$ (black circles) collected on the 8–50 GHz and 75–110 GHz NP measurements systems and the smoothed, continuous $\angle\Gamma_{s,opt}$ (solid line) processed from the raw NP sets. The frequency bands of the two independent NP measurement systems are indicated with the vertical dashed lines.

of the raw and smoothed NPs resulting from this technique. Here, the raw data collected on both the 8–50 GHz and the 75–110 GHz NP test benches are illustrated with black circles and the resulting smoothed data are illustrated with the solid black line.

It is clear that this approach provides a continuous set of NPs which can be interpolated to the 51–74 GHz frequency range where no raw measurements were collected. These resulting NPs can also be used for model extraction and validation across the entire broadband 8–110 GHz frequency range.

III. MILLIMETER-WAVE GAN HEMT TECHNOLOGIES

A total of six different mm-wave GaN HEMT technologies were characterized using the NP measurement systems outlined in Section II. Each transistor technology is described in the following subsections.

A. BAE SYSTEMS GAN09

BAE Systems developed a scaled device process targeting towards emerging applications at W-band [19]. The key features of this device technology are epitaxial structures based on vertically-scaled barrier layers and 90 nm T-gates with low parasitic capacitance. The epitaxial structure consisted of a 5 nm thick In $_{0.04}$ $Al_{0.7}Ga_{0.26}N$ barrier layer with a 1 nm thick AlN spacer layer and a 50 nm thick GaN channel. Structures contain an Al $_{0.04}$ $Ga_{0.96}N$ buffer layer to provide back-barrier carrier confinement which offers improvement to output conductance and device f_{max}. These devices typically have I_{max} of 1.8 A/mm and peak g_m exceeding 700 mS/mm. Measured S-Parameter data show f_T/f_{max} of 107/227 GHz respectively, demonstrating the feasibility of this technology to provide sufficient gain for power amplification up to high W-band frequencies. Devices were characterized for power performance at frequency of 94 GHz using a Maury passive load pull system at AFRL. At quiescent bias of $V_d = 10$ V and $I_d = 200$ mA/mm, GaN09 microstrip (MS) devices without an on-wafer pre-match demonstrated 3.3 W/mm with 30% PAE and 5.2 dB associated gain [19].

B. HRL LABORATORIES T3

HRL's T3 GaN HEMT is a commercially available 40 nm T-gate monolithic microwave integrated circuit (MMIC) foundry technology fabricated on a double heterostructure epitaxy consisting of an AlGaN cap, an AlN barrier, a GaN channel, and an AlGaN backbarrier, with a two-dimensional electron gas (2DEG) channel charge of 1.6×10^{13} cm $^{-2}$ and electron mobility of 1000 $cm^2/V\cdot$ s. The source and drain ohmic contacts are defined by selective-area n+ GaN MBE re-growth with a fixed spacing of 1.5 μm and a contact resistance of 0.1 Ω-mm between source-drain metal electrodes and the 2DEG. The typical dc and RF performance of the T3 GaN HEMT in production include 0.85 Ω-mm on-resistance, 1.4 A/mm maximum dc drain current density, 817 mS/mm peak transconductance, 72 V three-terminal breakdown voltage, f_T of 140 GHz, and Ka-band saturated output power of 2.7 W/mm at V_d of 14 V [20].

C. HRL LABORATORIES T3.5

HRL's T3.5 GaN HEMT is a 40 nm T-gate MMIC technology fabricated on the identical AlGaN/AlN/GaN/AlGaN double heterostructure epitaxy that is described in the T3 section. The T3.5 differs in the aggressive and adjustable scaling of the source-drain length, also defined by selective-area n+ GaN MBE ohmic regrowth. The regrowth scales from 1.5 μm to 0.15 μm (150 nm) on the same wafer, offering a continuum of FET access lengths that can be tailored to the desired application. T3.5 is a method of fabricating previously reported advanced T4 devices [21] in a fraction of the cycle time in a manner completely compatible with the T3 fabrication process. T3.5 essentially offers an additional degree of design freedom–the source-drain length–with its resulting performance advantages. The T3.5 devices reported in this article have a source-drain length of 0.25 μm (250 nm) with a centered 40-nm T-gate. The typical device characteristics are as follows: 2.3 A/mm maximum drain current density, 1.2 S/mm peak transconductance, 0.35 Ω-mm on-resistance, 15 V three-terminal breakdown voltage, 230 GHz cut-off frequency (f_t), 500 GHz maximum oscillation frequency (f_{max}), 3.1 W/mm saturated output power with 45% PAE at 94 GHz [22]. Recently, HRL published record performance at W-band of 56 % PAE with 780 mW/mm associated output power density [23].

D. HRL LABORATORIES T3L

HRL's T3L GaN FET is a graded-channel AlGaN/GaN device with the engineering of GaN device linearity and the peak electric field [24]. The device is fabricated as part of HRL's GaN MMIC technology. The device channel consists of a GaN layer and an Al-composition-graded AlGaN layer. The scaled graded-channel GaN offers the spreading of the electron carriers to form a quasi-3DEG. This was confirmed by measured capacitance vs. voltage curves of a graded-channel GaN HEMT structure [25]. An AlGaN barrier layer is grown on top of the graded AlGaN layer to reduce gate leakage. The graded-channel AlGaN/GaN HEMTs were grown by MOCVD on SiC substrate. The graded-channel AlGaN/GaN HEMTs show electron mobility of 1650–1000 cm ^{2}/V· s, depending on carrier density of 5×10^{12} - 1.2×10^{13} cm $^{-2}$, comparable to scaled conventional AlGaN/GaN HEMTs. The ohmic process was done with selective re-growth of n+ GaN by MBE, showing an ohmic contact resistance of 0.1 Ω-mm. With the source-to-drain spacing of 1.1 μm, the on-state resistance was about 0.9 Ω-mm. The 50 nm gate-length T-gate was fabricated with a mini field-plate for additional electric field engineering. The Imax was about 1.6 - 1.8 A/mm. HRL's T3L GaN recently demonstrated a record 45 % power added efficiency at 94 GHz [26] and 2 W W-band PA MMICs [27].

E. NORTHROP GRUMMAN CORPORATION GAN09

Northrop Grumman's (NG's) 90 nm GaN technology (GaN09) used for this study has been designed for V- and W-band operation. NG's GaN09 technology utilizes a 90 nm

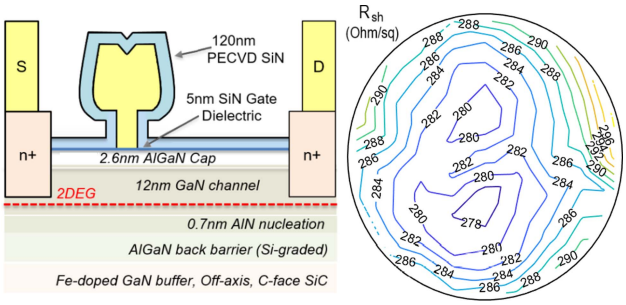

FIGURE 7. Cross-section of the Teledyne N-polar HEMTs reported (not to scale) and sheet resistance across wafer after deposition of 14 nm of PECVD SiNx.

T-gate without field plates. The epi-profile includes a back-barrier and a scaled Schottky barrier to minimize short channel effects. Parasitic resistances are reduced with the use of regrown n+ GaN for Ohmic contact formation. Typical Ohmic contact resistance is < 0.1 Ω-mm. Although discrete transistors were characterized, a full monolithic microwave integrated circuit process which includes metal-insulator-metal capacitors, thin film resistors, plated lines with airbridges, a 50 μm thick silicon carbide substrate, and slot thru-wafer-vias were used for fabrication.

F. TELEDYNE SCIENTIFIC N-POLAR GAN

Teledyne Scientific developed a nitrogen-polar (N-polar) GaN HEMT for RF power applications [28]. The cross-section of the planar HEMT device is illustrated in Fig. 7. The HEMT epitaxy was grown by MOCVD on a 100-mm SiC substrate [29]. The average sheet resistance of the structure obtained using Lehighton after deposition of an additional 14 nm of PECVD SiNx is also plotted in Fig. 7 and indicates 285 Ω/sq with a standard deviation of 5 Ω/sq. The device fabrication starts with the n++ GaN MOCVD regrowth process after hydrogen silsesquioxane (HSQ) patterning of the HEMT source-drain region for protection during regrowth. The film, composed of an unintentionally doped GaN and a highly Si-doped n++ GaN layer, is grown at a total thickness of 80 nm yielding a sheet resistance of 100 Ω/sq. Following Ohmic regrowth, ion implant of As+ and He+ species is used for device isolation. Prior to gate metal patterning, a 6.5 nm MOCVD SiNx gate dielectric is deposited, which is reduced to a nominal thickness of 5 nm following the gate metallization pre-treatment etch. A tri-layer E-Beam resist process is then utilized for patterning the gate metal electrode at a gate length of 80 nm. The HEMTs are oriented such that channel transport is perpendicular to the substrate miscut steps, ensuring that the device current flows in the highest mobility direction. For HEMT device passivation, a PECVD SiNx film is used at a thickness of 120 nm. Finally 0.6 μm of Au Ohmic overlay metallization is patterned, which also serves as probe pad metal.

Teledyne's N-Polar GaN HEMT has exhibited excellent RF power performance, including a highly uniform 100 mm wafer demonstration of 43% PAE and 2 W/mm at an 8 V drain bias at 94 GHz [23].

IV. MEASURED RESULTS

The noise and gain performance of the mm-wave GaN HEMT technologies are next investigated. The various GaN technologies were measured with two different VNA calibration algorithms depending on whether the samples included on-wafer calibration structures. The WinCal line-reflect-reflect-match (LRRM) algorithm [30] was used to measure transistors which did not include any on-wafer calibration structures. The reference planes of these measurements were therefore at the probe tips of the test benches. The multiline thru-reflect-line (mTRL) calibration algorithm [31] was used for measuring transistors which included on-wafer calibration structures. The reference planes of measurements collected using the mTRL calibration algorithm were at the ends of the thru line "launch" structures and are typically closer to the intrinsic device.

The mTRL calibration algorithm is widely regarded as the most accurate for on-wafer measurements [32]. This technique was utilized whenever possible. However, not all mm-wave GaN chips included on-wafer calibration structures. Therefore, special care was taken when analyzing measurements using different calibration algorithms as high frequency calibration is heavily affected by choice of the calibration algorithm [32], [33]. In this survey, the authors are careful not to directly compare the measurement results obtained using the two different calibration algorithms. The measured results in the remainder of this article will therefore be reported in two categories: measurements collected using the LRRM calibration algorithm and measurements collected using the mTRL calibration algorithm. It is also noted again that the LRRM calibrated measurements on the W-band NP test bench were collected with GGB WR-10 Picoprobes.

The minimum NF $\mathrm{NF_{min}}$ and associated gain G_{assoc} of the mm-wave GaN HEMT technologies were analyzed by collecting NP measurements using the methodology outlined in Section II. This manuscript reports the best performing device out of the small sample size collected from each foundry. The standard definitions for the measured NPs were reported in Section II. In order to assess the physicality of the measurements, the Wiatr-Pospieszalski (WP) parameter [34], [35] was computed and used as a criterion for filtering out inaccurate NP measurements.

A. LRRM CALIBRATED MEASUREMENTS

The first set of data include LRRM calibrated NP measurements of the three technologies in a coplanar waveguide (CPW) configuration without on-wafer calibration structures. These device configurations contain ground-signal-ground pads with short CPW transmission lines leading to the intrinsic transistors. The technologies in CPW configuration are the HRL T3, HRL T3.5, and the Teledyne N-Polar GaN HEMTs. The HRL T3 and T3.5 HEMTs were biased with $V_{DS} = 4$ V drain supply voltage and the Teledyne N-Polar

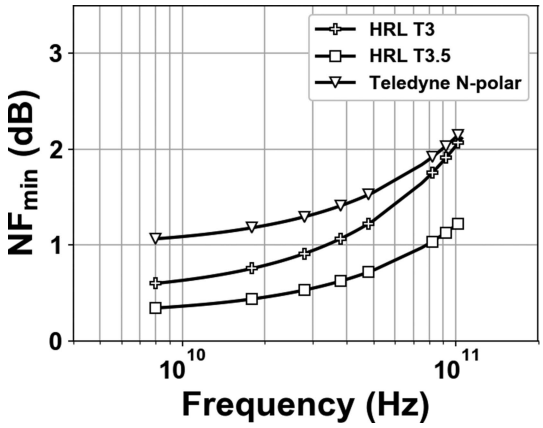

FIGURE 8. Measured NF_{min} of the HRL T3 (plus signs), HRL T3.5 (squares), and the Teledyne N-Polar (inverted triangles) GaN HEMT technologies as a function of frequency from 8–110 GHz. The LRRM calibration algorithm was used for measuring each CPW transistor.

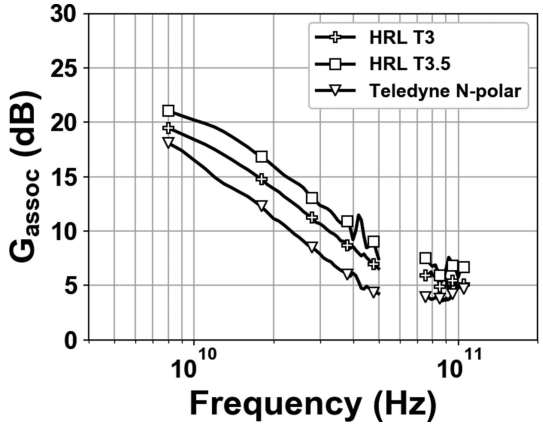

FIGURE 9. Measured G_{assoc} of the HRL T3 (plus signs), HRL T3.5 (squares), and the Teledyne N-Polar (inverted triangles) GaN HEMT technologies. The LRRM calibration algorithm was used for measuring each CPW transistor.

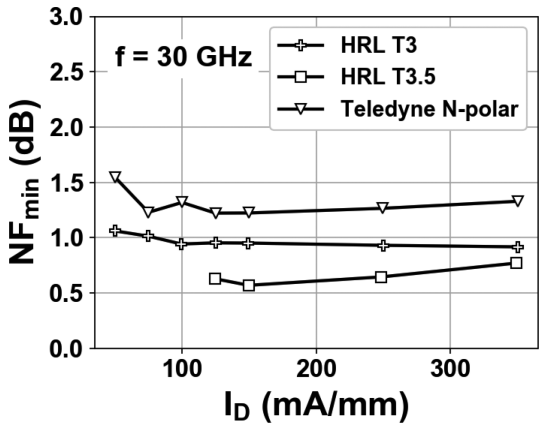

FIGURE 10. Measured NF_{min} at 30 GHz of the HRL T3 (plus signs), HRL T3.5 (squares), and the Teledyne N-Polar (inverted triangles) GaN HEMT technologies as a function of quiescent drain current. The HRL transistors were biased with a 4 V drain supply voltage and the Teledyne N-Polar GaN HEMT was biased with an 8 V drain supply voltage. The LRRM calibration algorithm was used for measuring each CPW transistor. Measurements which did not satisfy the WP parameter were excluded.

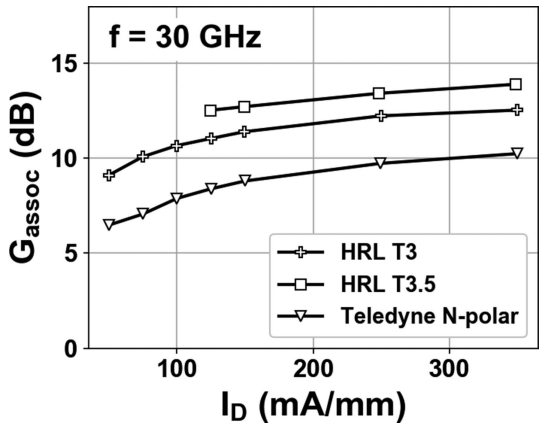

FIGURE 11. Measured G_{assoc} at 30 GHz of the HRL T3 (plus signs), HRL T3.5 (squares), and the Teledyne N-Polar (inverted triangles) GaN HEMT technologies as a function of quiescent drain current. The HRL transistors were biased with a 4 V drain supply voltage and the Teledyne N-Polar GaN HEMT was biased with an 8 V drain supply voltage. The LRRM calibration algorithm was used for measuring each CPW transistor. Measurements which did not satisfy the WP parameter were excluded.

GaN HEMT was biased with $V_{DS} = 8$ V drain supply voltage. Fig. 8 presents the smoothed NF_{min} measurements determined from the processed NPs across an ultra broadband 8–110 GHz frequency range and at a single quiescent bias. The associated gain of the CPW transistors as a function of frequency from 8–110 GHz is reported in Fig. 9. The transistor quiescent drain current used for these measurements was $I_D = 100$ mA/mm for each GaN HEMT technology. It is noted that G_{assoc} is not processed or smoothed during the raw NP post processing procedure.

The trade-off between minimum NF and associated gain is next analyzed for the LRRM calibrated NP measurements. This is enabled by measuring the NPs of each transistor at a single drain supply voltage and across a range of quiescent drain currents. The drain supply voltage of $V_{DS} = 4$ V is used for the HRL T3 and HRL T3.5 GaN HEMTs and a drain supply voltage of $V_{DS} = 8$ V is used for the Teledyne N-Polar GaN HEMT. The gate supply voltages are swept such that the transistors are biased at a quiescent drain current ranging from 25 mA/mm to 350 mA/mm in non-uniform steps. Fig. 10 presents the processed NF_{min} as a function of quiescent drain current for the two HRL and Teledyne GaN technologies at 30 GHz. Each technology exhibits excellent Ka-band minimum NF properties across a wide range of operating conditions. Fig. 11 reports the associated gain of each GaN technology as a function of quiescent drain current at 30 GHz. These results compare favorably to prior N-polar GaN NF reports including [36], where an NF_{min} of 1.6 dB was reported at 30 GHz.

The W-band noise and gain performance is also investigated using the ultra broadband NP measurements collected on the CPW GaN HEMTs. Fig. 12 illustrates the smoothed NF_{min} measurements as a function of quiescent drain current at 94 GHz. These results range from 1.1 dB to 2.1 dB NF_{min}–two excellent benchmarks at mm-wave frequencies. Fig. 13

TABLE 1. Summary of LRRM Calibrated Noise-Parameters and Gain at 30 GHz and 94 GHz and 150 mA/mm Quiescent Drain Current

					30 GHz				94 GHz			
Technology	W_G (μm)	L_G (nm)	V_{GS} (V)	V_{DS} (V)	NF_{min} (dB)	R_n (Ω)	$\Gamma_{s,opt}$	G_{assoc} (dB)	NF_{min} (dB)	R_n (Ω)	$\Gamma_{s,opt}$	G_{assoc} (dB)
HRL T3.5	2x37.5	40	-1.35	4.0	0.568	17.5	0.65∠47.7°	12.72	1.365	6.5	0.63∠141.7°	7.83
HRL T3	2x37.5	40	-0.63	4.0	0.95	27.2	0.7∠46.0°	11.4	1.961	9.0	0.59∠140.1°	5.78
Teledyne N-polar	2x37.5	80	-3.41	8.0	1.222	41.7	0.75∠42.9°	8.8	2.024	29.1	0.75∠121.1°	4.6

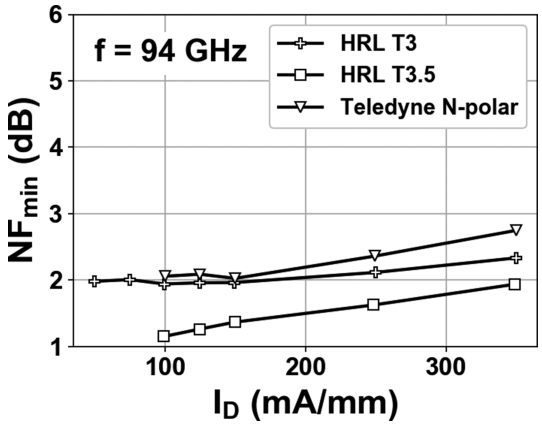

FIGURE 12. Measured NF_{min} at 94 GHz of the HRL T3 (plus signs), HRL T3.5 (squares), and the Teledyne N-Polar (inverted triangles) GaN HEMT technologies as a function of quiescent drain current. The HRL transistors were biased with a 4 V drain supply voltage and the Teledyne N-Polar GaN HEMT was biased with an 8 V drain supply voltage. The LRRM calibration algorithm was used for measuring each CPW transistor. Measurements which did not satisfy the WP parameter were excluded.

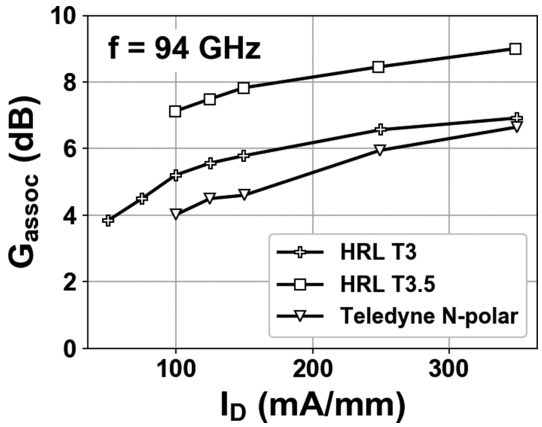

FIGURE 13. Measured G_{assoc} at 94 GHz of the HRL T3 (plus signs), HRL T3.5 (squares), and the Teledyne N-Polar (inverted triangles) GaN HEMT technologies as a function of quiescent drain current. The HRL transistors were biased with a 4 V drain supply voltage and the Teledyne N-Polar GaN HEMT was biased with an 8 V drain supply voltage. The LRRM calibration algorithm was used for measuring each CPW transistor. Measurements which did not satisfy the WP parameter were excluded.

reports the measured G_{assoc} as a function of quiescent drain current at 94 GHz. The wide range of low NF_{min} enables a good trade-off between high gain and NF for each of these technologies.

A summary of the LRRM calibrated NP measurements of the HRL T3, HRL T3.5 and Teledyne N-polar CPW transistors is reported in Table 1. Here, the measurements collected at the 150 mA/mm quiescent drain current are reported. The total device periphery, W_G and gate length, L_G, are reported in the table. It is evident from the measured results that each technology demonstrates excellent noise and gain performance at Ka-band and W-band frequencies. These results also provide a good benchmark for future low noise technology demonstrations at mm-wave frequencies.

B. mTRL CALIBRATED MEASUREMENTS

The next set of measured results include CPW and MS extended reference plane (ERP) transistors on die which included on-wafer calibration structures for the mTRL calibration algorithm. The three technologies in these device configurations were the BAE GaN09, the HRL T3L, and the NGSP GaN09 HEMTs.

The trade-off between minimum NF and associated gain is again analyzed across the quiescent drain current space. Each GaN HEMT technology was biased using a drain supply voltage of $V_{DS} = 4$ V, and the gate supply voltage was applied such that the quiescent drain current ranged from 25 mA/mm to 350 mA/mm in non-uniform steps. The smoothed NF_{min} as a function of quiescent drain current measured on the three ERP transistors at 30 GHz are reported in Fig. 14. Fig. 15 presents the measured G_{assoc} at 30 GHz from the mTRL calibrated NP measurements of the ERP transistors. These measurements provide excellent benchmarks for Ka-band low noise performance of mm-wave GaN HEMT technologies. Again, the W-band noise and gain performances of the mm-wave GaN HEMT technologies are analyzed. These metrics are extracted from the on-wafer mTRL calibrated 8–110 GHz NP measurements. Fig. 16 presents the smoothed NF_{min} at 94 GHz as a function of quiescent drain current for the three ERP GaN HEMTs. The measured G_{assoc} at 94 GHz of the ERP transistors are illustrated in Fig. 17. The three ERP GaN HEMT technologies exhibit excellent noise and gain performance across a wide range of quiescent drain currents at the $V_{DS} = 4$ V drain supply voltage.

A summary of the mTRL calibrated measurements of the BAE GaN09, the HRL T3L, and the NGSP GaN09 ERP GaN HEMTs is presented in Table 2. The quiescent drain current of each ERP transistor was 150 mA/mm for consistency in the summary. Each ERP GaN HEMT technology exhibits

TABLE 2. Summary of mTRL Calibrated Noise-Parameters and Gain at 30 GHz and 94 GHz and 150 mA/mm Quiescent Drain Current

					30 GHz				94 GHz			
Technology	W_G (μm)	L_G (nm)	V_{GS} (V)	V_{DS} (V)	$\mathrm{NF_{min}}$ (dB)	R_n (Ω)	$\Gamma_{\mathrm{s,opt}}$	G_{assoc} (dB)	$\mathrm{NF_{min}}$ (dB)	R_n (Ω)	$\Gamma_{\mathrm{s,opt}}$	G_{assoc} (dB)
BAE GaN09	2x25	90	-2.07	4.0	0.61	31.6	0.79∠32.5°	10.37	1.571	20.1	0.64∠100.4°	5.1
HRL T3L	4x37.5	50	-0.12	4.0	0.459	10.0	0.64∠66.2°	10.65	1.767	4.0	0.57∠166.8°	5.76
NGSP GaN09	4x25	90	-3.01	4.0	0.678	15.4	0.64∠42.3°	9.68	1.585	15.5	0.65∠122.4°	5.75

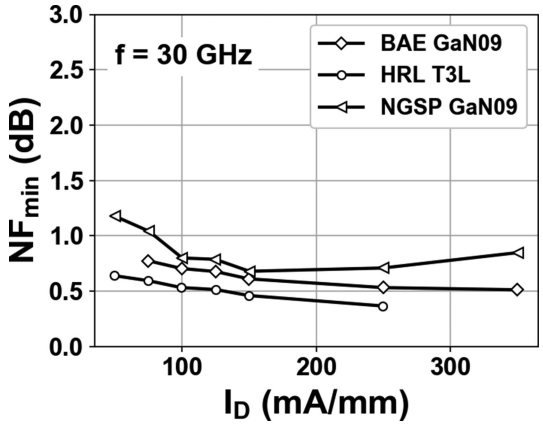

FIGURE 14. Measured $\mathrm{NF_{min}}$ at 30 GHz of the BAE GaN09 (diamonds), HRL T3L (circles), and the NGSP GaN09 (pentagons) GaN HEMT technologies as a function of quiescent drain current. Each transistor was biased using a 4 V drain supply voltage. The on-wafer mTRL calibration algorithm was used for measuring each ERP transistor. Measurements which did not satisfy the WP parameter were excluded.

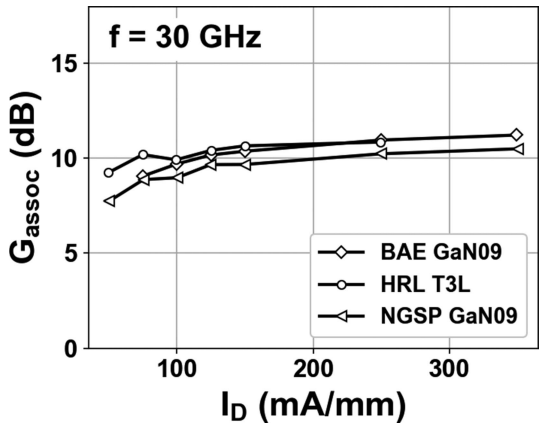

FIGURE 15. Measured G_{assoc} at 30 GHz of the BAE GaN09 (diamonds), HRL T3L (circles), and the NGSP GaN09 (pentagons) GaN HEMT technologies as a function of quiescent drain current. Each transistor was biased using a 4 V drain supply voltage. The on-wafer mTRL calibration algorithm was used for measuring each ERP transistor. Measurements which did not satisfy the WP parameter were excluded.

excellent Ka-band and W-band noise and gain performance. This summary also serves as a good reference for future mm-wave low noise technology developments and amplifier demonstrations.

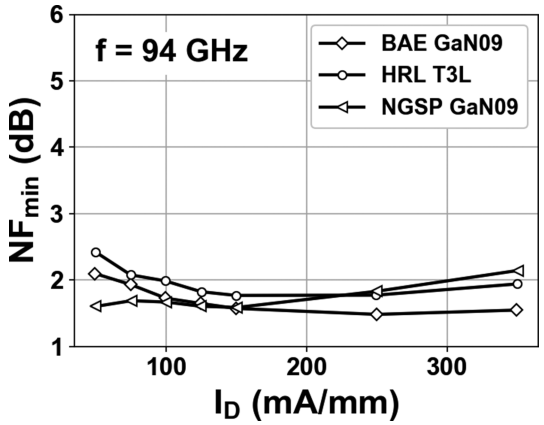

FIGURE 16. Measured $\mathrm{NF_{min}}$ at 94 GHz of the BAE GaN09 (diamonds), HRL T3L (circles), and the NGSP GaN09 (pentagons) GaN HEMT technologies as a function of quiescent drain current. Each transistor was biased using a 4 V drain supply voltage. The on-wafer mTRL calibration algorithm was used for measuring each ERP transistor.

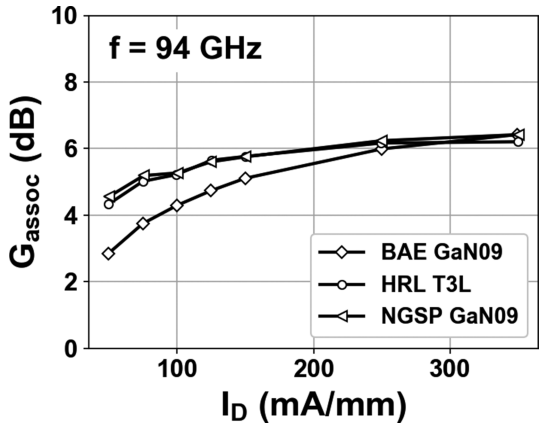

FIGURE 17. Measured G_{assoc} at 94 GHz of the BAE GaN09 (diamonds), HRL T3L (circles), and the NGSP GaN09 (pentagons) GaN HEMT technologies as a function of quiescent drain current. Each transistor was biased using a 4 V drain supply voltage. The on-wafer mTRL calibration algorithm was used for measuring each ERP transistor.

C. SMALL-SIGNAL MODEL ANALYSES

An extensive investigation of the measured NPs of both the CPW and ERP GaN HEMT technologies was presented in the previous section. To further aid in the analysis of the mm-wave GaN transistors, small-signal models were extracted and analyzed to shed light on the noise performance. Small-signal

TABLE 3. SSEC Model Parameters and Fukui Noise Calculations of the LRRM Calibrated CPW Transistor Measurements

Technology	C_{GS} (fF/mm)	C_{GD} (fF/mm)	C_{DS} (fF/mm)	R_{GS} (Ω-mm)	R_{GD} (Ω-mm)	R_{DS} (Ω-mm)	R_G (Ω-mm)	R_S (Ω-mm)	$G_{m,i}$ (mS/mm)	NF_{min} @ 94 GHz (dB)
HRL T3	358.7	130.1	136.5	2.46	2.38	18.47	0.7	0.75	617.4	1.815
HRL T3.5	289.2	131.6	167.0	3.37	1.42	29.77	0.45	0.14	599.9	1.041
Teledyne N-polar	531.4	128.6	78.0	0.04	0.94	100.27	0.29	0.07	266.7	1.989

The models were evaluated at the same quiescent drain voltage as Table 1 and at 100mA/mm quiescent drain current.

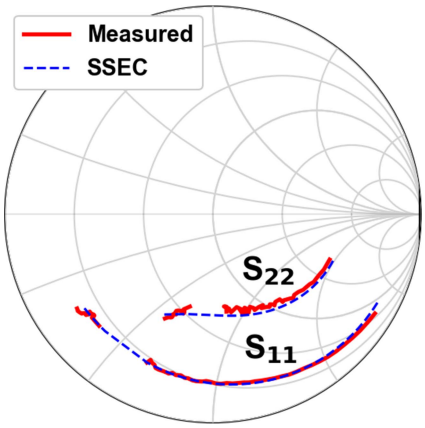

FIGURE 18. A comparison of the measured (red solid lines) and the SSEC simulated (blue dashed lines) S-Parameters of a GaN HEMT biased at 4 V drain supply voltage and 100 mA/mm quiescent drain current.

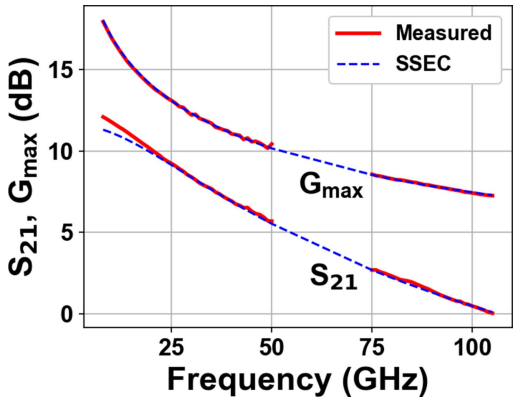

FIGURE 19. A comparison of the measured (red solid lines) and the SSEC simulated (blue dashed lines) S_{21} and maximum gain of a GaN HEMT biased at 4 V drain supply voltage and 100 mA/mm quiescent drain current.

equivalent circuit (SSEC) models were extracted from the S-Parameter measurements included with the NP measurements. This work employs the small-signal model developed by Lu et al. [37]. However, the analysis is not constrained to this particular SSEC model and could be accomplished with the various others that exist in the literature.

The first step in developing the SSEC model was extraction of the extrinsic parasitics. Cold field effect transistor (FET) measurements were employed for these purposes in a similar fashion to [37]. The pinch-off cold FET measurements were collected at varying gate supply voltages according to the threshold voltages of each mm-wave GaN HEMT technology. Next, the extrinsic parasitics were fed into custom SSEC extraction codes. These codes optimized the extrinsic parasitic components in order to ensure a quality fit of the SSEC S-Parameter simulations compared to the measured S-Parameters. This optimization process also ensures that the intrinsic components of the SSEC are flat versus frequency in a fashion similar to the work by Jarndal in [38]. An example of an extracted SSEC model compared to the S-Parameter measurements of a transistor is presented in Figs. 18 and 19. Here, the measured S-Parameters are plotted with solid red lines and the SSEC simulated S-Parameters are plotted with dashed blue lines. These comparisons provide confidence that the extracted SSEC model accurately represents the measured data. The SSEC models extracted for the complete set of mm-wave GaN HEMT technologies exhibited similar accuracy compared to the measurements.

The noise performance of the mm-wave GaN HEMT technologies is now investigated using the well-known Fukui minimum noise factor model [39],

$$F_{\min} = 1 + 2\pi K_f f C_{GS} \sqrt{\frac{R_G + R_S}{G_{m,i}}}, \tag{4}$$

where K_f is a fitting factor, f is frequency, C_{GS} is the SSEC intrinsic gate-source capacitance, R_G is the SSEC extrinsic gate resistance, R_S is the SSEC extrinsic source resistance, and $G_{m,i}$ is the SSEC intrinsic AC transconductance. The pertinent SSEC intrinsic and extrinsic parameters extracted from the measurements of each mm-wave GaN HEMT technology were fed into the analytic model for minimum NF. For this work, a fitting factor of $K_f = 1.6$ was employed to ensure good agreement between the calculated minimum NF and the measured equivalents. This fitting factor was used for evaluating each mm-wave GaN HEMT technology. The fitting factor used in this work could be useful for future evaluations of mm-wave GaN HEMT technologies as it is different than what was reported in [39].

A summary of the SSEC model parameters and the Fukui model minimum NFs are reported in Tables 3 and 4. A 100 mA/mm quiescent drain current was used for evaluating

TABLE 4. SSEC Model Parameters and Fukui Noise Calculations of the On-Wafer mTRL Calibrated ERP Transistor Measurements

Technology	C_{GS} (fF/mm)	C_{GD} (fF/mm)	C_{DS} (fF/mm)	R_{GS} (Ω-mm)	R_{GD} (Ω-mm)	R_{DS} (Ω-mm)	R_G (Ω-mm)	R_S (Ω-mm)	$G_{m,i}$ (mS/mm)	$\mathrm{NF_{min}}$ @ 94 GHz (dB)
BAE GaN09	470.6	194.5	173.5	0.88	0.31	17.65	0.3	0.27	498.2	1.695
HRL T3L	507.4	131.3	140.4	0.49	1.4	11.63	0.28	0.18	656.1	1.473
NGSP GaN09	570.7	150.8	138.2	0.09	0.6	20.66	0.24	0.14	532.3	1.632

The models were evaluated at the same quiescent drain voltage as Table 1 and at 100mA/mm quiescent drain current.

each GaN HEMT technology. The simple Fukui model indicates that NF is minimized when the transistor's gate-source capacitance, gate resistance, and source resistance are minimized while maximizing the intrinsic AC transconductance. In the case of the LRRM calibration measurements of the CPW transistors, the HRL T3.5 GaN HEMT exhibited the lowest combination of C_{GS}, R_G, and R_S while simultaneously exhibiting the highest $G_{m,i}$. Out of the mTRL calibrated measurements of ERP transistors, the BAE GaN09 and NGSP GaN09 HEMTs exhibited an excellent minimization of the C_{GS}, R_G, and R_S parameters while maintaining good $G_{m,i}$. These model results provide first-order quantitative insight into the mm-wave noise and gain performances of the GaN HEMT technologies that were analyzed in this survey.

V. CONCLUSION

This work provided a set of measured benchmarks for noise and gain performance of mm-wave GaN HEMT technologies used in Ka-band and W-band frequency ranges. In particular, six different mm-wave GaN HEMTs were measured on two NP test benches from 8–50 GHz and 75–110 GHz. The resulting raw NP measurements were stitched together to yield smoothed NPs across an ultra broadband 8–110 GHz. Comparisons of the smoothed minimum NF and associated gain were presented for the transistors measured with LRRM and on-wafer mTRL calibrations. Excellent minimum NF and associated gain were observed in the various GaN HEMTs characterized in this article.

ACKNOWLEDGMENT

The authors from Pseudolithic gratefully recognize the guidance and support of program manager Dr. Paul Maki. The authors from Teledyne Scientific acknowledge the support of Ron Birkhahn from Transphorm Inc, and thank the Teledyne Scientific Clean Room staff for the device fabrication. The HRL research was developed with funding from the Defense Advanced Research Projects Agency (DARPA). The views, opinions and/or findings expressed are those of the author and should not be interpreted as representing the official views or policies of the Department of Defense or the U.S. Government.

REFERENCES

[1] U. K. Mishra, L. Shen, T. E. Kazior, and Y.-F. Wu, "GaN-based RF power devices and amplifiers," *Proc. IEEE*, vol. 96, no. 2, pp. 287–305, Feb. 2008. [Online]. Available: https://ieeexplore.ieee.org/document/4414367/

[2] S. Lardizabal, K. C. Hwang, J. Kotce, A. Brown, and A. Fung, "Wideband W-band GAN LNA MMIC with state-of-the-art noise figure," in *Proc. IEEE Compound Semicond. Integr. Circuit Symp.*, 2016, pp. 1–4. [Online]. Available: httpss://ieeexplore.ieee.org/document/7751079/

[3] K. W. Kobayashi and V. Kumar, "A broadband 70–110-GHz E-/W-band LNA using a 90-nm T-gate GaN HEMT technology," *IEEE Microw. Wireless Compon. Lett.*, vol. 31, no. 7, pp. 885–888, Jul. 2021. [Online]. Available: httpss://ieeexplore.ieee.org/document/9417206/

[4] R. Malmqvist et al., "A W-band single-chip receiver in a 60 nm GaN-on-silicon foundry process," in *Proc. IEEE 16th Eur. Microw. Integr. Circuits Conf.*, Apr. 2022, pp. 51–54. [Online]. Available: https://ieeexplore.ieee.org/document/9784092/

[5] X. Tong et al., "A 22–30 GHz GAN low-noise amplifier with 0.4–1.1-dB noise figure," *IEEE Microw. Wireless Compon. Lett.*, vol. 29, no. 2, pp. 134–136, Feb. 2019.

[6] C. Florian, P. A. Traverso, and A. Santarelli, "A Ka-band MMIC LNA in GAN-on-Si 100-nm technology for high dynamic range radar receivers," *IEEE Microw. Wireless Compon. Lett.*, vol. 31, no. 2, pp. 161–164, Feb. 2021.

[7] K. W. Kobayashi, V. Kumar, C. Campbell, S. Chen, and Y. Cao, "18-44GHz K/Ka-band robust-35.5 dBm reconfigurable 90nm GaN HEMT LNA," in *Proc. IEEE BiCMOS Compound Semicond. Integr. Circuits Technol. Symp.*, 2020, pp. 1–4.

[8] S.-Y. Chen, C.-S. Wu, L.-Y. Lee, T.-H. Chen, Y.-M. Chen, and H. Wang, "25-31-GHz low noise amplifiers in 0.15-μm GAN/SIC HEMT process," in *Proc. IEEE Int. Symp. Radio-Freq. Integration Technol.*, 2022, pp. 27–29.

[9] M. Micovic et al., "Ka-band LNA MMIC's realized in Fmax> 580 GHz GaN HEMT technology," in *Proc. IEEE Compound Semicond. Integr. Circuit Symp.*, 2016, pp. 1–4.

[10] F. Thome, P. Bruckner, S. Leone, and R. Quay, "A wideband E/W-band low-noise amplifier MMIC in a 70-nm gate-length GaN HEMT technology," *IEEE Trans. Microw. Theory Techn.*, vol. 70, no. 2, pp. 1367–1376, Feb. 2022. [Online]. Available: https://ieeexplore.ieee.org/document/9662226/

[11] S. Masuda et al., "GaN MMIC amplifiers for W-band transceivers," in *Proc. Eur. Microw. Conf.*, 2009, pp. 1796–1799. [Online]. Available: https://ieeexplore.ieee.org/document/5295964/

[12] X. Tong, P. Zheng, and L. Zhang, "Low-noise amplifiers using 100-nm gate length GaN-on-silicon process in W-band," *IEEE Microw. Wireless Compon. Lett.*, vol. 30, no. 10, pp. 957–960, Oct. 2020. [Online]. Available: https://ieeexplore.ieee.org/document/9189934/

[13] I. Kallfass et al., "A highly linear 84 GHz low noise amplifier MMIC in AlGaN/GaN HEMT technology," in *Proc. IEEE MTT-S Int. Microw. Workshop Ser. Millimeter Wave Integr. Technol.*, 2011, pp. 144–147. [Online]. Available: https://ieeexplore.ieee.org/document/6061860/

[14] R. Weber et al., "A beyond 110 GHz GaN cascode low-noise amplifier with 20.3 dBm output power," in *Proc. IEEE/MTT-S Int. Microw. Symp.*, 2018, pp. 1499–1502. [Online]. Available: https://ieeexplore.ieee.org/document/8439698/

[15] T. Sonnenberg, A. Romano, S. Verploegh, M. Pinto, and Z. Popović, "*V*- and *W*-band millimeter-wave GaN MMICs," *IEEE J. Microwaves*, vol. 3, no. 1, pp. 453–465, Jan. 2023.

[16] S. A. Maas, *Noise in Linear and Nonlinear Circuits*. Norwood, MA, USA: Artech House, 2005.

[17] L. Dunleavy, "Application note 033: Understanding noise parameter measurements," 2023. [Online]. Available: www.modelithics.com

[18] G. Simpson, D. Ballo, J. Dunsmore, and A. Ganwani, "A new noise parameter measurement method results in more than 100x speed improvement and enhanced measurement accuracy," in *Proc. 72nd ARFTG Microw. Meas. Symp.*, 2008, pp. 119–127. [Online]. Available: https://ieeexplore.ieee.org/document/4804299/

[19] P. Srivastava et al., "90 nm GaN technology for millimeter-wave power applications to W-band and beyond," in *Proc. Device Res. Conf.*, 2023, pp. 1–2.
[20] G. Siddiqi et al., "Improving manufacturability of highly scaled RF GaN HEMTs," in *Proc. Int. Conf. Compound Semicond. Manuf. Technol.*, 2022, pp. 65–68. [Online]. Available: https://csmantech.org/wp-content/acfrcwduploads/field_5e8cddf5ddd10/post_6286/4.4_Improving_manufacturability.pdf
[21] K. Shinohara et al., "Scaling of GaN HEMTs and schottky diodes for submillimeter-wave MMIC applications," *IEEE Trans. Electron Devices*, vol. 60, no. 10, pp. 2982–2996, Oct. 2013. [Online]. Available: https://ieeexplore.ieee.org/document/6553129
[22] D. Denninghoff et al., "High-efficiency GaN MMIC technology for W-band applications and beyond," in *Proc. Eur. Microw. Week Workshop WS03 Millimeter-Wave GaN Power Amplifiers*, Sep. 2022, pp. 1–2. [Online]. Available: https://www.eumweek.com/archive/eumweek2022/www.eumweek.com/conferences/Workshops-Short-Courses.html
[23] F. E. Arkun et al., "W-band fully passivated AlN/GaN HEMT device with 56% power-added efficiency and 780 mW/mm output power density at 94 GHz," in *Proc. Device Res. Conf.*, 2023, pp. 1–2, doi: 10.1109/DRC58590.2023.10187016.
[24] J.-S. Moon et al., "Power scaling of graded-channel GaN HEMTs with mini-field-plate T-gate and 156 GHz fT," *IEEE Electron Device Lett.*, vol. 42, no. 6, pp. 796–799, Jun. 2021.
[25] J.-S. Moon et al., "360 GHz fmax graded-channel AlGaN/GaN HEMTs for mmW low-noise applications," *IEEE Electron Device Lett.*, vol. 41, no. 8, pp. 1173–1176, Aug. 2020.
[26] J.-S. Moon et al., "W-band graded-channel GaN HEMTs with record 45% power-added-efficiency at 94 GHz," *IEEE Microw. Wireless Technol. Lett.*, vol. 33, no. 2, pp. 161–164, Feb. 2023.
[27] J.-S. Moon et al., "High-power density W-band MMIC amplifiers using graded-channel GaN HEMTs," in *Proc. IEEE/MTT-S Int. Microw. Symp.*, 2023, pp. 97–100.
[28] A. Arias et al., "High performance N-polar GaN HEMTs with OIP3/Pdc 12dB at 10GHz," in *Proc. IEEE Compound Semicond. Integr. Circuit Symp.*, 2017, pp. 1–3.
[29] D. Bisi et al., "Commercially available N-polar GaN HEMT epitaxy for RF applications," in *Proc. IEEE 8th Workshop Wide Bandgap Power Devices Appl.*, 2021, pp. 250–254.
[30] L. Hayden, "An enhanced line-reflect-reflect-match calibration," in *Proc. 67th ARFTG Conf.*, Jun. 2006, pp. 143–149. [Online]. Available: https://ieeexplore.ieee.org/document/4734364/
[31] R. B. Marks, "A multiline method of network analyzer calibration," *IEEE Trans. Microw. Theory Techn.*, vol. 39, no. 7, pp. 1205–1215, Jul. 1991. [Online]. Available: https://ieeexplore.ieee.org/document/85388/
[32] A. Rumiantsev and N. Ridler, "VNA calibration," *IEEE Microw. Mag.*, vol. 9, no. 3, pp. 86–99, Jun. 2008. [Online]. Available: https://ieeexplore.ieee.org/document/4519498/
[33] N. C. Miller, M. Elliott, E. Lam, R. Gilbert, J. Uyeda, and R. L. Coffie, "Improving the precision of on-wafer W-band scalar load-pull measurements," *IEEE J. Microwaves*, vol. 3, no. 3, pp. 1005–1013, Jul. 2023.
[34] M. W. Pospieszalski, "Interpreting transistor noise," *IEEE Microw. Mag.*, vol. 11, no. 6, pp. 61–69, Oct. 2010.
[35] L. Boglione, "Considerations on the $4NT_o/t_m$ ratio and the noise correlation matrix of active and passive two-port networks," *IEEE Trans. Microw. Theory Techn.*, vol. 61, no. 12, pp. 4145–4153, Dec. 2013.
[36] M. Guidry et al., "Improved N-polar GaN mm-wave linearity, efficiency, and noise," in *Proc. IEEE/MTT-S Int. Microw. Symp.*, 2022, pp. 291–294.
[37] J. Lu, Y. Wang, L. Ma, and Z. Yu, "A new small-signal modeling and extraction method in AlGaN/GaN HEMTs," *Solid-State Electron.*, vol. 52, no. 1, pp. 115–120, Jan. 2008. [Online]. Available: https://linkinghub.elsevier.com/retrieve/pii/S0038110107002511
[38] A. Jarndal and G. Kompa, "A new small-signal modeling approach applied to GaN devices," *IEEE Trans. Microw. Theory Techn.*, vol. 53, no. 11, pp. 3440–3448, Nov. 2005. [Online]. Available: https://ieeexplore.ieee.org/document/1528795/
[39] H. Fukui, "Optimal noise figure of microwave GaAs MESFET's," *IEEE Trans. Electron Devices*, vol. 26, no. 7, pp. 1032–1037, Jul. 1979. [Online]. Available: https://ieeexplore.ieee.org/document/1480119/

NICHOLAS C. MILLER (Senior Member, IEEE) received the B.S., M.S., and Ph.D. degrees in electrical and computer engineering from Michigan State University, East Lansing, MI, USA, in 2013, 2015, and 2017, respectively. He is currently an Electronics Engineer with the Air Force Research Laboratory Sensors Directorate, Dayton, OH, USA. He is also a young professional member of the IEEE MTT-3 Microwave Measurements Committee. His technical research interests include broad range of fundamental, applied, and computational physics, applied mathematics, electrical engineering, linear and nonlinear RF characterization, and linear and nonlinear RF modeling and simulation. Dr. Miller was the recipient of the IEEE AP-S pre-doctoral research Award in 2013, U.S. DoD science, mathematics, and research for transformation (SMART) scholarship in 2014, IEEE Dayton Section Harrell V. Nobel Award in 2019 for physics-based device modeling, Best Conference Paper Award at the 21st IEEE Wireless and Microwave Technology Conference (WAMICON) in 2021, and Best Presentation Award at the IEEE MTT-S Young Professional Workshop on Optimization and Modeling of Active Devices in 2022.

ANDREA ARIAS-PURDUE (Member, IEEE) received the B.S. and M.S. degrees in theoretical physics from California State University at Fresno, Fresno, CA, USA, in 2007 and 2009, respectively. She has six years of experience in semiconductor device development and yield improvement for high voltage applications, which includes developing drift step recovery diodes with less than 5 ns half-width and greater than 8 kV V_p, and developing the technology under DARPA's microscale power conversion program, which enabled 1 GHz switching demonstration for a GaN-based GHz speed dc–dc power converter. Her current research interests include high power millimeter-wave HEMT development and efficiency enhancement techniques for broadband operation. She was the recipient of the American Physical Society Kennedy Reed Award (Best Theoretical Research) in 2009, second prize, for her work on the temporal contributions to the Wentzel–Kramers–Brillouin-like calculation of the radiation that results from space-time field quantization that is detected by a non-inertial observer.

ERDEM ARKUN (Member, IEEE) received the B.S. degree in materials science and engineering from Middle East Technical University, Ankara, Turkey, in 1999, and the M.S. and Ph.D. degrees from North Carolina State University, Raleigh, NC, USA in 2002 and 2006, respectively. From 2006 to 2009, he was a Postdoctoral Associate with the University of Minnesota, Minneapolis, MN, USA, and later with the University of Santa Barbara, Santa Barbara, CA, USA. He was with Translucent Inc. from 2009 to 2015 and with Teledyne Imaging Sensors from 2015 to 2018. He has been with HRL Laboratories, where he is the lead of epitaxial materials for RF GaN electronics.

DAVID BROWN (Member, IEEE), photograph and biography not available at the time of publication.

JAMES F. BUCKWALTER (Fellow, IEEE) received the B.S.E.E. degree (Hons.) in electrical engineering from the California Institute of Technology (Caltech), Pasadena, CA, USA, in 1999, the M.S. degree from the University of California-Santa Barbara (UCSB), Santa Barbara, CA, in 2001, and the Ph.D. degree in electrical engineering from Caltech, in 2006. He is currently a Professor of electrical and computer engineering with UCSB. He has co-founded Pseudolithic as the Chief Design Officer.

ROBERT L. COFFIE (Senior Member, IEEE) received the B.S. degree in engineering physics from the University of Oklahoma, Norman, OK, USA, in 1997, and the Ph.D. degree in electrical and computer engineering from the University of California, Santa Barbara, CA, USA, in 2003. He is currently a Senior Staff Engineer of microelectronic semiconductors with Northrop Grumman. He has designed, developed, and matured AlGaN/GaN HEMT technologies for RF applications from L-band to Q-band with Northrop Grumman and TriQuint Semiconductor (now Qorvo). He also developed the first JEDEC qualified AlGaN/GaN HEMTs for 600 V power switching applications with Transphorm, where he was the Director of Device Engineering. He holds 13 patents and has authored more than 30 journal articles related to AlGaN/GaN HEMTs, a book chapter on new materials for high power RF applications, and the book *2D Electrostatics* (CRC Press, 2021).

ANDREA CORRION (Member, IEEE) received the bachelor's degree in materials science and engineering from the University of Michigan, Ann Arbor, MI, USA, in 2002, and the M.S. and Ph.D. degrees from the University of California, Santa Barbara, CA, USA, in 2008. She joined HRL Laboratories as a member of the Technical Staff in 2008 and has been a Principal Investigator and Program Manager for a number of programs related to GaN HEMTs and also a Group Manager and Department Manager for RF MMIC Technologies and RF Materials and Devices departments. Since May 2022, she has also been the Director of the Microfabrication Technologies Laboratory, HRL.

DANIEL J. DENNINGHOFF (Member, IEEE) received the B.S. degree in electrical and computer engineering from the U.S. Air Force Academy, El Paso, CO, USA, in 2004, the M.S. degree in electrical and computer engineering from the Air Force Institute of Technology, Dayton, OH, USA, in 2006, and the Ph.D. degree in electrical and computer engineering from the University of California at Santa Barbara, Santa Barbara, CA, USA, in 2012. He leads all RF GaN activity with HRL Laboratories. His technical career include Principal Investigator and Program Manager positions with HRL, Qorvo, Teledyne, Transphorm, AFRL, and his own start-ups. Prior to his technical career, he was an Air Force freefall parachute instructor and jumpmaster. He has conducted research, development, and commercialization of low-noise, high-efficiency, high-frequency, and high-power GaN HEMTs, MMICs, and modules for RF and power conversion applications. He holds ten patents and has authored or coauthored more than 40 papers. He was the recipient of the Best Student Paper Award for his demonstration of nitrogen-polar GaN HEMTs with record-setting f_{max} at the 2012 Device Research Conference.

MICHAEL ELLIOTT is curerntly working toward the undergraduation degree in electrical engineering with Arizona State University, Tempe, AZ, USA. He has been with Air Force Research Laboratory in the electrical field for more than ten years since 2006. He is currently an RF Test Technician. His work specializes in passive and active load pull, noise parameter measurements, millimeter wave measurements, and large and small signal device characterizations. He is committed to continual growth.

DAVE FANNING (Senior Member, IEEE) received the B.S. degree in physics from the Massachusetts Institute of Technology, Cambridge, MA, USA, and the Ph.D. degree from the University of Illinois, Urbana and Champaign, IL, USA, focused in condensed matter physics and materials development. He is currently the Group Lead for RF Device Technologies. At Qorvo (TriQuint), he worked in the areas of GaN and GaAs process development working in Technical and Program Manager roles on several customer, DARPA, AFRL, and ONR funded programs. He pioneered III-V field plate technology and processed spanning from S- to W-band for commercial and defense applications. He was also with Lockheed Martin's Missiles and Fire Control, where he was able to deploy GaN devices at the system level and demonstrate state of the art RF GaN power. He was the RF Seeker Hardware Lead for the Miniature Hit-to-Kill program and was the Subject Matter Expert on GaN RF technology and semiconductor foundry interface for Lockheed overall. At HRL, his research focuses on maturing the T3 GaN process and advancing the generation of wide bandgap processes.

RYAN GILBERT received the Bachelor of Science degree in electronics engineering technology from DeVry University, Naperville, IL, USA. He has been a contractor, working on site with AFRL, since 2010. He is currently a Senior RF Test Engineer, specializing in active and passive load pull, millimeter wave measurements, vector signal analysis, and small and large signal characterization. Before joining AFRL, his background included designing and constructing RF resonators for MRI research.

DANIEL S. GREEN (Member, IEEE) received the B.S. degree in physics and electrical engineering from Yale University, New Haven, CT, USA, in 1998, and the M.S. and Ph.D. degrees in electrical and computer engineering from the University of California, Santa Barbara, Santa Barbara, CA, USA, in 2000 and 2006, respectively. He recently joined the Office of Naval Research, Arlington, VA, USA, as a Program Officer. He was with RF Micro Devices, where he worked to develop gallium nitride technology. He has extensive experience in both growth and characterization of GaN heterostructure materials. He has also done significant work in GaN radio-frequency device development, including device design, fabrication, and reliability measurement. Dr. Green is a member of the Materials Research Society, IEEE Microwave Theory and Technology Society, and IEEE Electron Devices Society.

FLORIAN HERRAULT (Senior Member, IEEE) received the B.S. and M.S. degrees in physics and materials science from the National Institute of Applied Sciences (INSA), Toulouse, France, in 2003 and 2005, respectively, and the Ph.D. degree in electrical and electronics engineering from the University of Toulouse, Toulouse, in 2009. From 2009 to 2013, he was a Research Engineer and the Deputy Director with the MicroSensors and MicroActuators Group, Georgia Institute of Technology, Atlanta, GA, USA. He has been with HRL Laboratories, LLC, Malibu, CA, USA, where he is currently the Group Leader of Advanced Packaging Solutions for mm-wave, E/O, and IR subsystems. He has co-founded Pseudolithic as the Chief Technical Officer.

BEN HEYING, photograph and biography not available at the time of publication.

CASEY M. KING (Member, IEEE) has more than 25 years of experience in the semiconductor industry and is currently a member of the Technical staff with Teledyne Scientific for advanced process development of GaN high-electron-mobility transistor technology.

EYTHAN LAM (Member, IEEE) received the B.S. degree in electrical engineering in 2020 from the University of California, Santa Barbara, Santa Barbara,CA, USA, where he is currently working toward the Ph.D. degree. His research focuses on high-efficiency power amplifier design in upper millimeter wave bands and predistortion.

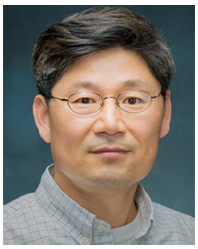

JEONG-SUN MOON (Fellow, IEEE) is currently a Principal Scientist with HRL Laboratories, Malibu, CA, USA. Since 2000, he has been with HRL and a PI for numerous contracts from DARPA, ONR, JPL, and NASA. At HRL, his research focuses on emerging materials, novel devices, RF circuits, and electro-optic applications. Before joining the HRL, he was with Sandia National Laboratories. He has authored or coauthored three book chapters and more than 200 papers and holds 30 patents. He was the recipient of the 2014 George Abraham Outstanding Paper Award from Government Microcircuit Applications and Critical Technology Conference (GOMACTech), and NASA SPACE ACT Board Award in 2009. He was an editor of a top-notch IEEE journal and IEEE ELECTRON DEVICE LETTERS. He also gave numerous invited conference and workshop presentations and tutorials/short courses. His work was featured in various magazines including, *IEEE Spectrum, Compound Semiconductor*, *NASA Tech Briefs, Microwave Journal*, and *MIT Technology Review*. He served on the Program Committee for the Device Research Conference. He is a member of the Technical Program Committee of the Microwave Theory and Techniques Society (MTT-S).

PETRA V. ROWELL (Member, IEEE), photograph and biography not available at the time of publication.

GEORGES SIDDIQI (Member, IEEE) received the B.S. degree in chemical engineering from the University of California, Los Angeles, Los Angeles, CA, USA, in 2007, the M.S. degree from UC Berkeley, Berkeley, CA, USA, in 2010, and the D.Sc. degree in chemistry from ETH Zurich, Zurich, Switzerland, in 2016. After a Postdoc with Yale focusing on ALD deposition, he has been with RF GaN since 2017, first with Northrop Grumman from 2017 to 2020, followed by HRL Laboratories, LLC since 2020. At HRL, he is the Responsible Scientific Authority for GaN, and a task lead and Principal Investigator on several DoD programs.

IOULIA SMORCHKOVA, photograph and biography not available at the time of publication.

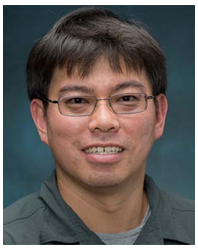

JOE TAI received the B.S. and M.S. degrees in electrical engineering from the University of California, Los Angeles, Los Angeles, CA, USA, in 2004 and 2008, respectively. Since 2012, he has been with HRL as an RF Engineer, specializing in millimeter wave measurement, compact device model for GaN device, and MMIC design.

JANSEN UYEDA received the B.S. degree in electrical engineering from the University of Hawai'i, Honolulu, Hawaii, and the M.S. degree in electrical engineering from the University of Southern California, Los Angeles, CA, USA. In 1997, he joined Northrop Grumman Space Systems (previously T.R.W. Space & Electronics), Redondo Beach, CA, USA, as a member of Technical Staff, where he was responsible for lithography operations in the GaAs HBT and HEMT production line. He is currently a Senior Staff Engineer, supporting development and maturation of GaN technologies.

MIKE WOJTOWICZ, photograph and biography not available at the time of publication.